

Supplementary Information for: “Structural differences between toxic and nontoxic HypF-N oligomers” by Claudia Capitini, Jayneil R. Patel, Antonino Natalello, Cristiano D’Andrea, Annalisa Relini, James A. Jarvis, Leila Birolo, Alessia Peduzzo, Michele Vendruscolo, Paolo Matteini, Christopher M. Dobson, Alfonso De Simone, Fabrizio Chiti

SUPPLEMENTARY METHODS:

Protein expression, purification and mutagenesis. Wild-type and mutated forms of HypF-N were prepared and purified as described previously,¹ and stored at $-80\text{ }^{\circ}\text{C}$ in 20 mM potassium phosphate buffer, pH 7.0, with 2 mM dithiothreitol (DTT) (for the wild-type form) or in 100 mM potassium phosphate buffer, pH 7.0, with 2 mM tris(2-carboxyethyl)phosphine hydrochloride (TCEP) (for the mutated forms). ^{15}N - ^{13}C isotopically labelled HypF-N used in the NMR measurements was expressed in minimal medium as previously described,² and purified using the same protocol as for non-isotopically labelled samples.

Mutational variants of HypF-N, each carrying a single cysteine residue, were generated as described previously.¹ The sequence of wild-type HypF-N contains three cysteine residues located at positions 7, 40 and 65. The data reported here were obtained by using two double mutants of HypF-N (C7S/C40S and C7S/C65A), each, therefore, having a single cysteine residue at positions 65 and 40, respectively, and ten different quadruple mutants carrying a single cysteine residue located at different positions along the protein chain: $\Delta\text{Cys/T5C}$, $\Delta\text{Cys/Q10C}$, $\Delta\text{Cys/Q18C}$, $\Delta\text{Cys/F25C}$, $\Delta\text{Cys/N34C}$, $\Delta\text{Cys/E55C}$, $\Delta\text{Cys/V59C}$, $\Delta\text{Cys/E75C}$, $\Delta\text{Cys/Q83C}$, $\Delta\text{Cys/T89C}$.

Labelling of HypF-N variants with 1,5-IAEDANS and 6-IAF. Each of the 12 single cysteine variants of HypF-N was diluted to give a final protein concentration of 180 μM in 100 mM potassium phosphate buffer, pH 7.0, 3 M guanidine hydrochloride (GdnHCl). 45 μL of a 30 mM stock solution of 5-((((2-iodoacetyl)amino)ethyl)amino)naphthalene-1-sulfonic acid (1,5-IAEDANS) dye or 30 μL of a 30 mM stock solution of 6-iodoacetamidofluorescein (6-IAF) dye (Thermo Fisher Scientific, Waltham, MA, USA) dissolved in dimethylformamide (DMF) was added to give a final sample volume of 500 μL , in order to obtain a 15- and 10-fold molar excess of 1,5-IAEDANS and 6-IAF, respectively. The conditions were 180 μM protein, 2.7 mM 1,5-IAEDANS, 3 M GdnHCl, 100 mM potassium phosphate buffer, pH 7.0 for the experiments involving labelling with 1,5-IAEDANS, and 180 μM protein, 1.8 mM 6-IAF, 3 M GdnHCl, 100 mM potassium phosphate buffer, pH 7.0 for those involving the labelling with 6-IAF. Both types of reaction mixtures (one containing 1,5-IAEDANS and one containing 6-IAF) were left in the dark on a mechanical shaker for 2 h at $30\text{ }^{\circ}\text{C}$, then kept overnight in the dark while shaking at $4\text{ }^{\circ}\text{C}$. The labelled samples were dialysed in the dark (using a membrane with a cut-off of 3000 Da) against (i) 0.25 L of 100 mM potassium phosphate buffer, pH 7.0, with 1.5 M GdnHCl for 4 h, (ii) 0.25 L of 100 mM potassium phosphate buffer, pH 7.0 for 4 h, (iii) 0.5 L of 50 mM potassium phosphate buffer, pH 7.0, overnight, (iv) 1.0 L of 20 mM or 5 mM potassium phosphate buffer (depending on whether the labelled mutants were used to produce type A or type B oligomers, respectively), at pH 7.0, for 6 h. The samples were then centrifuged to remove any precipitate. The concentration of the dye in each 1,5-IAEDANS-labelled variant and in each 6-IAF-labelled variant was determined spectrophotometrically, using $\epsilon_{336} = 5700\text{ M}^{-1}\text{cm}^{-1}$ and $\epsilon_{491} = 8200\text{ M}^{-1}\text{cm}^{-1}$, respectively. The protein concentration was determined spectrophotometrically using $\epsilon_{336} = 12490\text{ M}^{-1}\text{cm}^{-1}$ after subtraction of the absorbance contribution of the 1,5-IAEDANS/6-IAF probe at the same wavelength of 280 nm. To estimate this contribution, the following equations were used:

$$y = 0.00247 + 0.00012436x \quad \text{for the 1,5-IAEDANS-labelled variants} \quad (1)$$

$$y = -0.017948 + 0.0037404x \quad \text{for the 6-IAF-labelled variants} \quad (2)$$

where x represents the molar concentration of the dye, and y is the absorbance value of the dye at 280 nm. The degree of labelling of the sample was then estimated by determining the ratio between the two measured dye and protein concentrations. In the FRET experiments described below, 1,5-IAEDANS and 6-IAF acted as donor and acceptor, respectively.

Preparation of HypF-N oligomers. Oligomeric aggregates of HypF-N were prepared by incubating the wild-type protein for 4 h at 25 °C without agitation and at a concentration of 48 μ M under two different experimental conditions: (i) 50 mM acetate buffer, 12% (v/v) trifluoroethanol (TFE), 2 mM DTT, pH 5.5 (condition A) and (ii) 20 mM trifluoroacetic acid (TFA), 330 mM NaCl, pH 1.7 (condition B). For the FRET experiments, type A and type B oligomers formed by each variant labelled with the donor dye 1,5-IAEDANS at position x and each variant labelled with the acceptor dye 6-IAF at position y (named x D_ y A) were produced, maintaining a constant molar ratio between donor-labelled variant and acceptor-labelled variant of 1:1 (24 μ M of x D and 24 μ M of y A). Oligomers x D_wt (with the acceptor-labelled variant replaced by wild-type HypF-N) and wt_ y A (with the donor-labelled variant replaced by wild-type HypF-N), where labelled and unlabelled HypF-N were in a 1:1 molar ratio, were also produced.

Tapping-mode atomic force microscopy (TM-AFM). Wild-type HypF-N type A and type B oligomers, obtained as described above, were centrifuged at 16,100 rcf for 10 min and then resuspended in potassium phosphate buffer, pH 7.0. For AFM inspection, a 10 μ L aliquot of each sample was diluted 100 times, deposited on a freshly cleaved mica substrate and dried *in vacuo*. TM-AFM images were acquired in air using a Dimension 3100 SPM equipped with “G” scanning head (maximum scan size 100 μ m) and driven by a Nanoscope IIIa controller, and a Multimode SPM equipped with “E” scanning head (maximum scan size 10 μ m) and driven by a Nanoscope V controller (Digital Instruments-Bruker). Single beam uncoated silicon cantilevers (type OMCL-AC160TS, Olympus) were used. The drive frequency was between 320 and 340 kHz and the scan rate was 0.5-2.0 Hz.

Fourier transform infrared (FTIR) spectroscopy. FTIR spectra of type A and type B HypF-N oligomers were recorded in attenuated total reflection (ATR) mode on a single reflection diamond element (Specac, UK) as previously described.³ Briefly, a 2 μ L aliquot of the protein solution was deposited on to the ATR plate and dried at room temperature to obtain a semi-dry film.^{3,4} Spectra were collected using a Varian 670-IR spectrometer (Varian Australia Pty Ltd, Mulgrave, Australia) equipped with a nitrogen-cooled mercury cadmium telluride detector under the following conditions: 25 kHz scan speed, 2 cm^{-1} spectral resolution, 1000 scans co-addition and triangular apodization. Second derivative spectra were obtained by the Savitzky-Golay method after a binomial smoothing of the absorption spectra.⁵ Curve fitting of the Amide I band (from 1700 to 1600 cm^{-1} , mainly attributable to the absorption of C=O peptide bonds) was performed as previously described⁶ using the GRAMS/32 (Galactic Industries Corporation, Salem, NH, USA) software.

Raman spectroscopy. Raman spectra of type A and type B HypF-N oligomers were acquired by means of a micro-Raman spectrometer (Xplora, Horiba Scientific, Lille, France) working in a backscattering geometry and equipped with a laser diode tuned at 638 nm as excitation wavelength. The investigated samples were prepared by drop-casting a 20 μL volume of 50 μM oligomer on a cleaned microscope glass slide, followed by air-drying at room temperature. The Raman scattered signal was obtained by focusing the laser beam to a ~ 7 μm diameter spot on the sample through a 10 \times objective (Olympus, NA 0.25) (measured power at the sample 2.4 mW) and then acquired by a Peltier-cooled CCD. The Raman spectra displayed represent the average of 20 measurements from different sample positions. Amide I spectral region (1600-1700 cm^{-1}) was analysed by curve fitting using the ORIGIN software (OriginLab Corp., Northampton, MA, USA).

ThT fluorescence spectroscopy. The tinctorial properties of HypF-N oligomers under conditions A and B, formed by wild-type HypF-N, as well as by each 1,5-IAEDANS-labelled variant and the unlabelled wild-type protein in a 1:1 molar ratio (xD_wt), were investigated using fluorescence spectroscopy. After the aggregation process, the oligomer samples containing a total protein concentration of 48 μM were centrifuged for 10 min at 16,100 rcf and the pellets were resuspended in 5 mM potassium phosphate buffer at pH 7.0. Aliquots (60 μL) of HypF-N aggregates were then added to 440 μL of a solution of 25 μM thioflavin T (ThT) in 25 mM phosphate buffer at pH 6.0, in order to keep a 3.7-fold molar excess of the dye. The intensity of the ThT fluorescence emission signal at 485 nm (excitation at 440 nm) was recorded at 25 $^{\circ}\text{C}$ by using a Perkin-Elmer LS 55 spectrofluorimeter (Wellesley, MA, USA) equipped with a thermostated cell-holder attached to a Haake F8 water-bath (Karlsruhe, Germany), and a 2 \times 10 mm quartz cell. The ratios between the ThT emission in the presence (F) and absence (F_0) of HypF-N oligomers were determined, and as negative controls the experiments were repeated using 24 μM soluble 1,5-IAEDANS-labelled L-glutathione (GSH).

Magic angle spinning (MAS) solid-state NMR (ssNMR) spectroscopy. MAS-ssNMR experiments were carried out on uniformly $^{13}\text{C}/^{15}\text{N}$ labelled type A and type B HypF-N oligomers on a 14.1T Bruker Avance III-HD Spectrometer with a 3.2 mm E-free probe (Bruker, Coventry, UK) at a temperature of 298 K. Dipolar-assisted rotational resonance (DARR)⁷ experiments were recorded at a spinning rate of $\nu_r = 10$ kHz using a mixing time of 20 ms, and the spectra were acquired using a 1 ms ^1H - ^{13}C cross polarisation (CP) contact time with RF fields of $\nu_{\text{RF}} = 55$ kHz on ^{13}C , and $\nu_{\text{RF}} = 67.5$ kHz on ^1H . Heteronuclear experiments (NCO and NCA) were acquired at a spinning rate of $\nu_r = 12.5$ kHz using double cross polarisation (DCP) experiments.⁸ The ^1H - ^{15}N CP condition was met with $\nu_{\text{RF}} = 45$ kHz for ^{15}N , and $\nu_{\text{RF}} = 57$ kHz for ^1H , and ^{15}N - ^{13}C CP was achieved with a ^{15}N RF field of $\nu_{\text{RF}} = 43.75$ kHz and a ^{13}C RF field of $\nu_{\text{RF}} = 18.75$ kHz for 6ms. For all DARR and DCP experiments, decoupling was applied using SPINAL-64 at $\nu_{\text{RF}} = 100\text{kHz}$ during t_1 evolution and acquisition, and the complex data were acquired using the States-TPPI method.⁹ For ^1H - ^{13}C Insensitive Nuclei Enhanced by Polarization Transfer (INEPT) spectra,¹⁰ a MAS frequency of $\nu_r = 10$ kHz was used, pulse widths were 2.5 μs for ^1H and 5.5 μs for ^{13}C , and ^1H TPPM decoupling was applied at $\nu_{\text{RF}} = 71.4\text{-}100$ kHz. Analysis of all spectra was made using CCPN analysis.¹¹

The ^1H - ^{13}C INEPT spectrum of the nontoxic oligomers was sequentially assigned using an additional edited- ^1H - ^{13}C INEPT spectrum where peaks from $-\text{CH}_2$ groups appear with an inverted phase from $-\text{CH}_3$ and $-\text{CH}$ groups. This was achieved using a refocused INEPT pulse sequence with delays of $1/4J_{\text{CH}}$ to generate polarisation on ^{13}C , and $3/8J_{\text{CH}}$ during the refocussing period, with $J_{\text{CH}}=140\text{Hz}$, as previously reported.¹² With the additional knowledge of the protonation state of each ^{13}C atom, ^1H and ^{13}C protein chemical shift statistics from the BMRB were used to assign all resonances in the spectrum to the backbone and sidechain resonances of the amino acids G, S, A, K, N

and T. Inspection of the HypF-N primary sequence revealed the 6 N-terminal residues as the only contiguous stretch of sequence consistent with the assignment.

1,5-IAEDANS and 6-IAF emission spectra. The oligomers xD_yA, xD_wt and wt_yA were formed at a total monomer concentration of 48 μ M, and then diluted in 20 mM and 5 mM potassium phosphate buffer (for type A and type B oligomers, respectively), pH 7.0, in order to obtain a final HypF-N monomer concentration of 2 μ M. Fluorescence emission spectra were recorded on a Perkin-Elmer LS 55 spectrofluorimeter (Wellesley, MA, USA) equipped with a thermostated cell-holder attached to a Haake F8 water-bath (Karlsruhe, Germany). The measurements were performed using a 2 \times 10 mm quartz cell at 25 °C with excitation at 336 nm. Emission spectra of 48 μ M native, non-aggregated, 1,5-IAEDANS- and 6-IAF-labelled HypF-N variants were also acquired. The FRET measurements between a donor-labelled residue (1,5-IAEDANS-labelled residue) and an acceptor-labelled residue (6-IAF-labelled residue) in type A and type B oligomers were determined as described in Fig. S8.

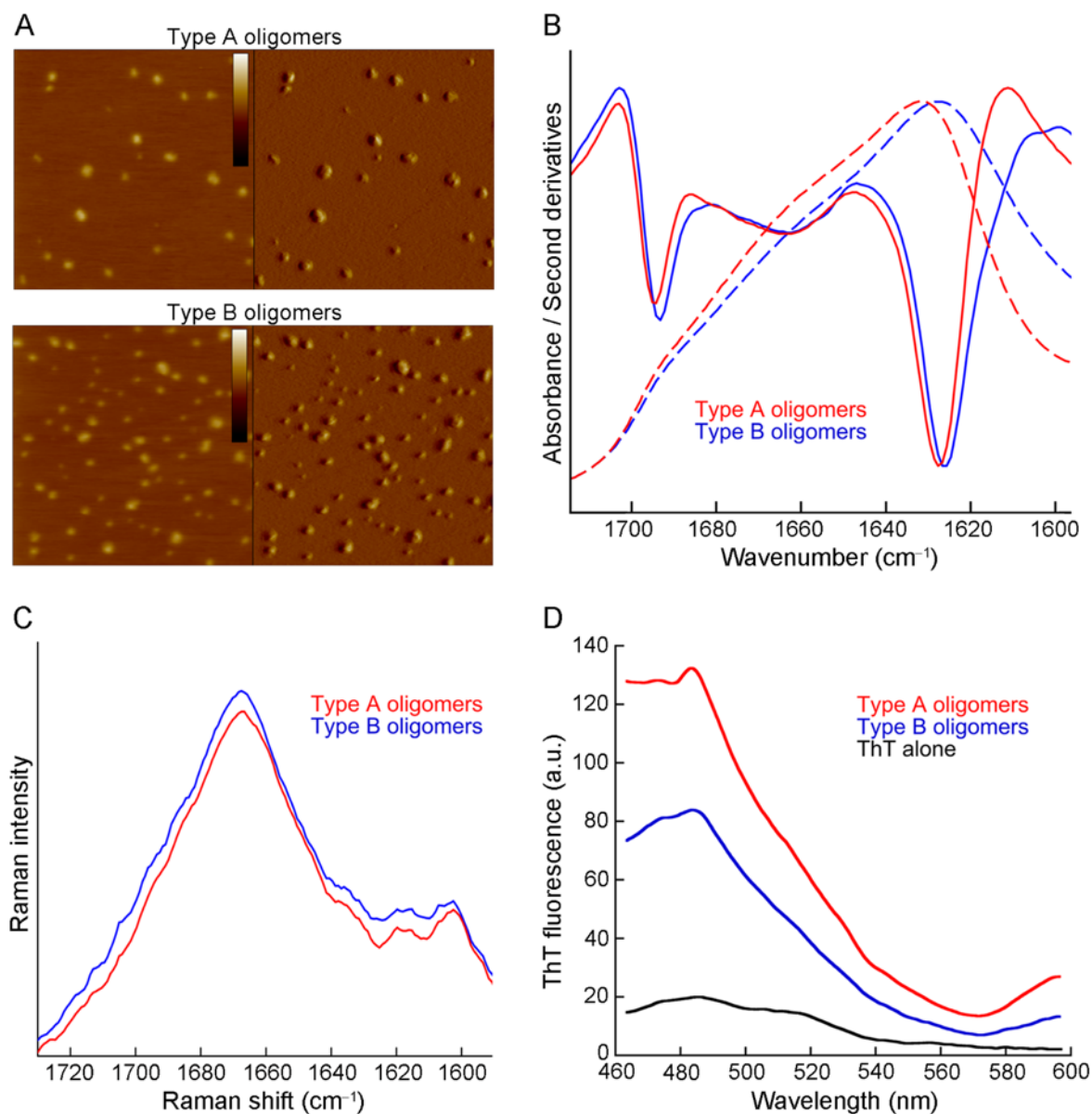
Limited proteolysis. Proteolysis of HypF-N oligomers was performed at 25 °C in 10 mM sodium phosphate, pH 7.0, with either trypsin at a 1:5000 (w/w) enzyme-to-substrate ratio, chymotrypsin at a 1:10000 (w/w) enzyme-to-substrate ratio, or proteinase K at a 1:1000 (w/w) enzyme-to-substrate ratio. The time course of proteolysis was monitored by sampling the reaction mixture at different time intervals (from 3 to 45 min). The reaction was stopped by adding 1 μ L of the peptide mixture to 1 μ L of MALDI matrix, 10 mg/mL α -cyano-4-hydroxycinnamic acid in 70% acetonitrile, 30% 50 mM citric acid, on a metallic sample plate for MALDI analysis. MALDI-TOF mass spectrometry (MS) analyses were performed on a Voyager DE STR Pro instrument operating in linear mode (Applied Biosystems, Framingham, MA, USA). Mass calibration was performed using a peptide standard mixture provided by the manufacturer. Acceleration and reflector voltages were set up as follows: the target voltage at 20 kV, the first grid at 66% of the target voltage, delayed extraction at 200 ns. All mass values are reported as average masses, and the raw data were analysed using software provided by the manufacturer.

Chemical exchange saturation transfer (CEST) measurements. CEST measurements were carried out at 10 °C under sample conditions that optimise the lag phase prior to extensive monomer depletion. For type A oligomers, these conditions were 50 mM acetate buffer, 10% (v/v) TFE, 2 mM DTT, pH 5.5, and for type B oligomers, they were 2 mM TFA, 330 mM NaCl, pH 1.7. The experiments were performed using a 16.85T Bruker Avance III-HD Spectrometer with TCI cryoprobe (Bruker, Coventry, UK), and were based on ^1H - ^{15}N -HSQC experiments by applying continuous wave saturation in the ^{15}N channel. As the exchange is probed between monomeric HypF-N (having sharp resonances) and the slow tumbling oligomeric states (having broad resonances), a series of large offsets ranging from ± 1.5 kHz to ± 10.0 kHz ($-10, -7.5, -5, -4.5, -4, -3.5, -3, -2.5, -2, -1.5, 0, 1.5, 2, 2.5, 3, 3.5, 4, 4.5, 5, 7.5$ and 10 kHz) were used to saturate the ^1H - ^{15}N -HSQC spectrum of HypF-N using a single B_1 field of bandwidth of 350 Hz. An additional spectrum with saturation at -100 kHz was recorded as a reference. CEST ^1H - ^{15}N -HSQC spectra were collected using a data matrix consisting of 2048 ($t_2, ^1\text{H}$) \times 440 ($t_1, ^{15}\text{N}$) complex points and spectral widths of 16.02 (^1H) and 20.0 ppm (^{15}N). CEST spectra were collected at increasing RF offsets and processed using nmrPIPE.¹³ Intensity values of each cross peak were obtained by using CCPNAnalysis.¹⁴ Each assigned peak at each offset was then compared to its reference spectrum at $+100$ kHz to give I/I_0 values and plotted against the residue number.

Structural modelling. Schematic representations of type A and type B HypF-N oligomers were obtained by using molecular dynamics (MD) simulations in implicit solvent. Initial models of the

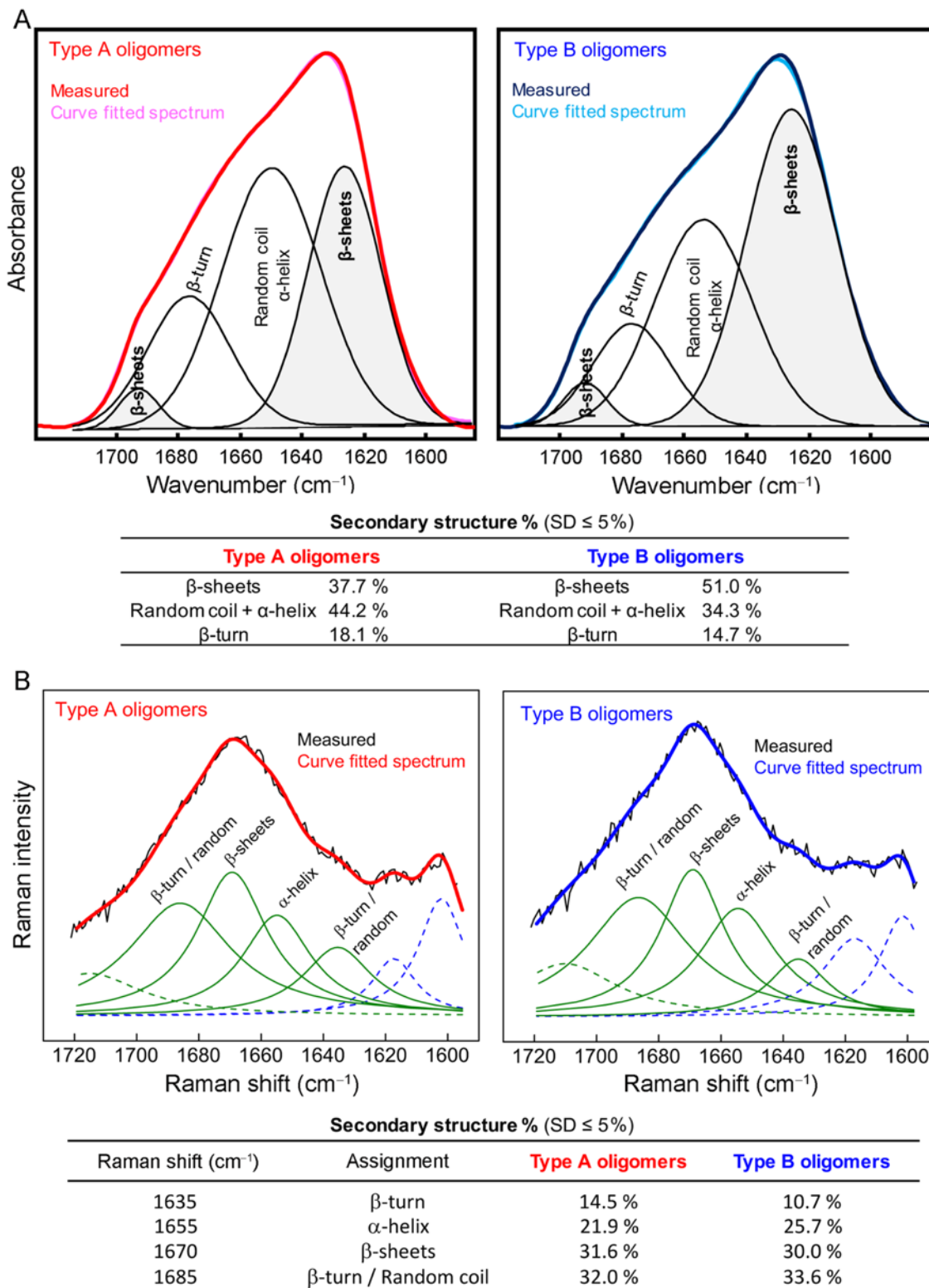
oligomers were made using rotation and translation of identical copies of the native structure of HypF-N. MD simulations at 500 K were run for 100 ns by restraining the Cartesian coordinates of the main chain in some structured β -sheet regions, by restraining 24 and 18 residues in type A and B oligomers, respectively. A final refinement has been run with 10 ns unrestrained simulations. In the case of type B, the N-terminal region was pulled with a constant force that was orthogonal to the main plane of the oligomers.

SUPPLEMENTARY RESULTS:



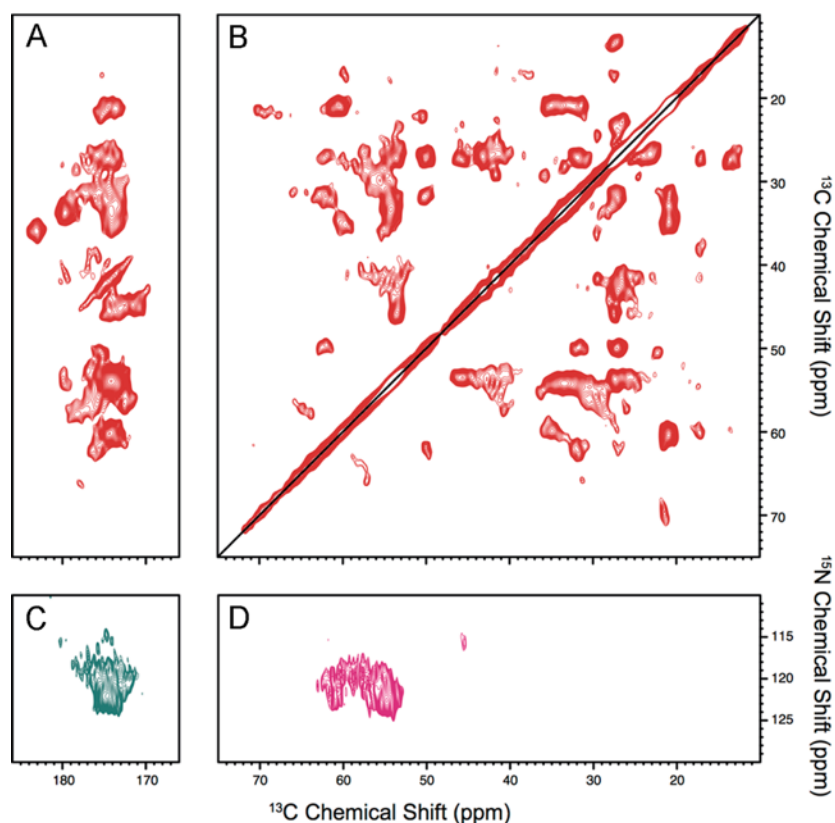
Supplementary Figure 1. (A) TM-AFM images (left, height data; right, amplitude data) of HypF-N samples revealed the presence of spherical bead-like aggregates with heights in the ranges of 2-6 nm and 2-7 nm under conditions A (top) and B (bottom), respectively. Scan size, 500 nm. The color scale corresponds to a Z range of 8 nm. (B) FTIR spectra in the Amide I band (dashed lines) showed a major component in the Amide I band at ~ 1631 cm⁻¹ and at ~ 1627 cm⁻¹ for type A (red) and B (blue) oligomers, respectively, which, along with a shoulder around 1694 cm⁻¹, were assigned to β -sheet secondary structure.¹⁵ These peaks can be observed more clearly in the second derivative spectra (continuous lines) whose minima correspond to absorption maxima, where they are found at ~ 1627 cm⁻¹ and ~ 1694 cm⁻¹ for type A oligomers (red) and at ~ 1626 cm⁻¹ and ~ 1693 cm⁻¹ for type B oligomers (blue). In addition, a broad component at ~ 1660 cm⁻¹ and a shoulder at ~ 1677 cm⁻¹ are observed in

both cases, attributable to a combination of random coil and β -turn structures. **(C)** Raman intensity spectra in the Amide I region ($1600\text{-}1720\text{ cm}^{-1}$) of type A (red) and type B (blue) HypF-N oligomers (smoothed raw data). The spectra of the two species are largely superimposable, indicating a similar distribution of secondary structure types for both species. Moreover, the presence in both cases of a major component at $\sim 1670\text{ cm}^{-1}$ confirms the predominance of β -sheet structure observed by the FTIR measurements described above. **(D)** ThT fluorescence emission spectra (excitation 440 nm) in the absence (black line) and in the presence of type A (red line) and type B (blue line) HypF-N oligomers. Both types of oligomers bind ThT and increase its fluorescence by *ca.* 6.5 and 4 fold for type A and B oligomers, respectively; this difference suggests that the β -sheet structure is more organised and more compact in type A oligomers compared to type B. These morphological, structural and tinctorial characteristics are in a very good agreement with those found previously.¹

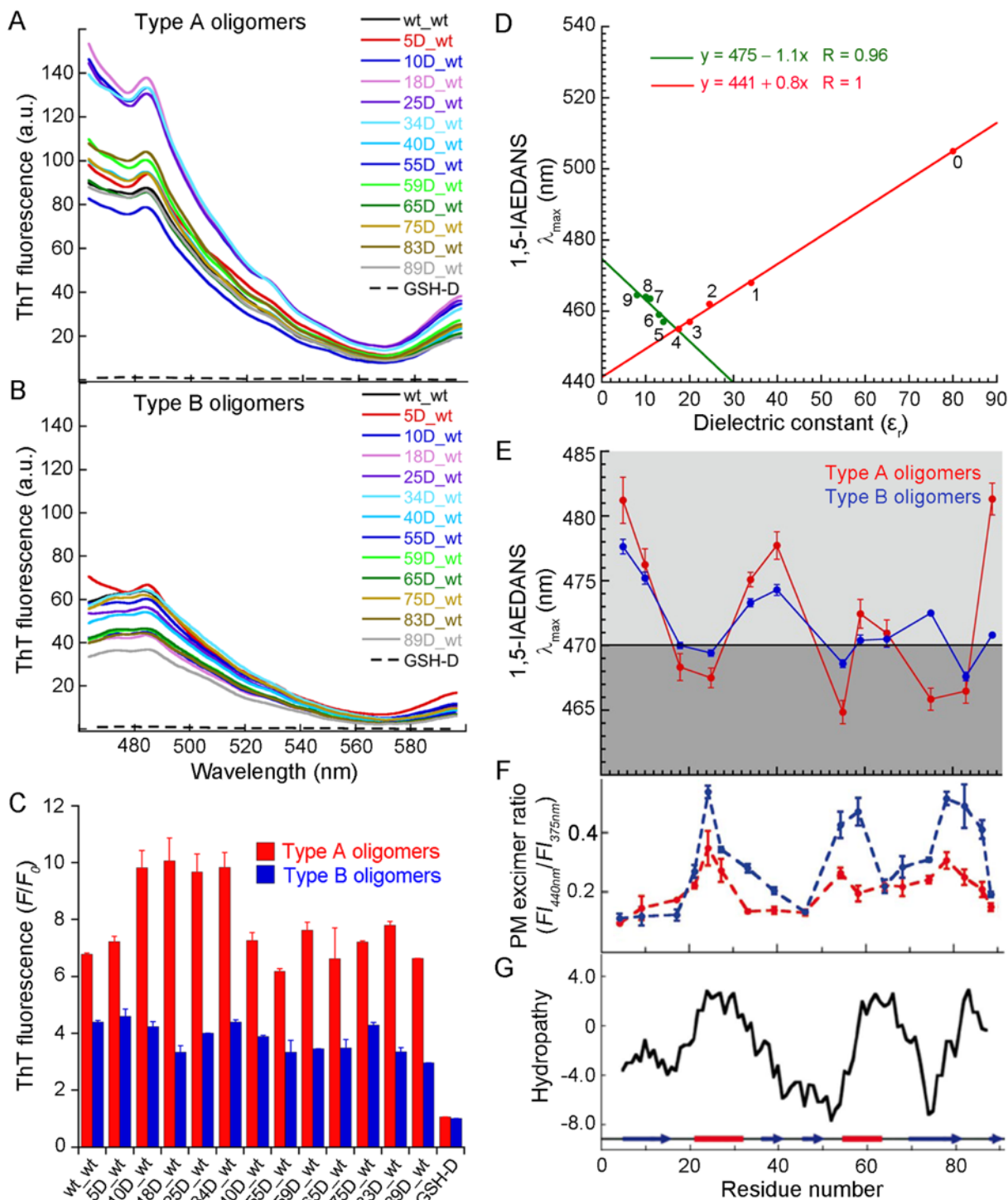


Supplementary Figure 2. Curve fitting analysis of the FTIR absorption (A) and the Raman scattering (B) spectra of type A (left) and type B (right) HypF-N oligomers within the 1600-1700 cm^{-1} range. In both cases, percentages of secondary structure types are reported in the tables below. The analysis of

the FTIR absorption spectra as a linear combination of Gaussian components reveals the presence of β -sheet, random coil and β -turn structures for both oligomer types. The Raman spectra analysis confirms the presence of the same secondary structure types observed with FTIR and a similar content of β -sheet and β -turns for both oligomer types, and, in addition, provides an estimate of the α -helix contribution,¹⁶ which is identified as a shoulder centered at 1655 cm^{-1} in both oligomer samples and accounts of about 24% of their total secondary structure content. Raman spectroscopy also provides information on amino acid residues in the regions below 1620 cm^{-1} and beyond 1700 cm^{-1} , accounting for the stretching modes of the aromatic rings of Tyr and Phe (blue dashed lines) and of the COO^- of Glu (green dashed line).

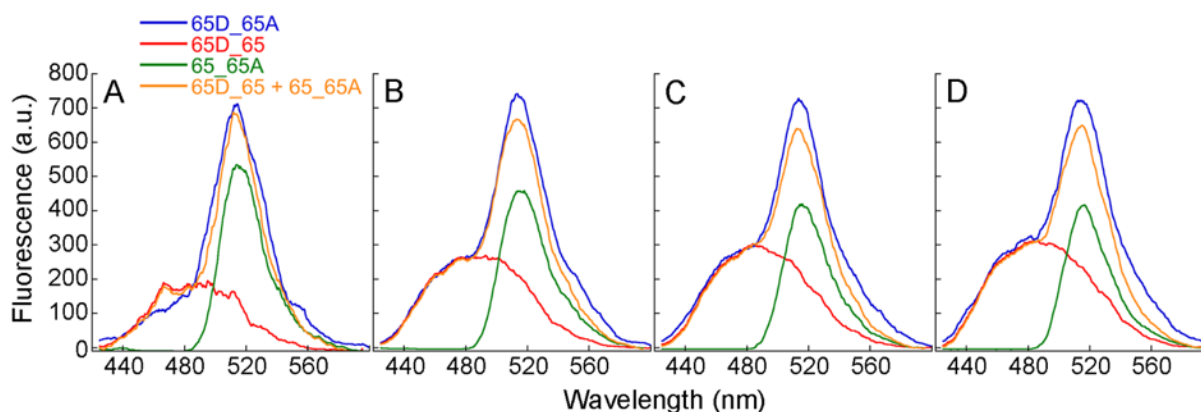


Supplementary Figure 3. Cross polarisation experiments with type A HypF-N oligomers. Correlations between various spin systems in the oligomers, as acquired in cross polarisation experiments, are shown in the different panels. (A,B) ^{13}C - ^{13}C DARR at a mixing time of 20 ms. Correlations are shown between carbonyl and aliphatic groups within the same residue (A) and between aliphatic groups of the same residue (B). (C,D) Heteronuclear ^{13}C - ^{15}N correlation spectra obtained for type A oligomers. Amide N and carbonyl C correlations (residues *i* and *i*-1, respectively) were measured using NCO experiments (C). Amide N and $\text{C}\alpha$ correlations (intra-residue) were measured using NCA experiments (D).

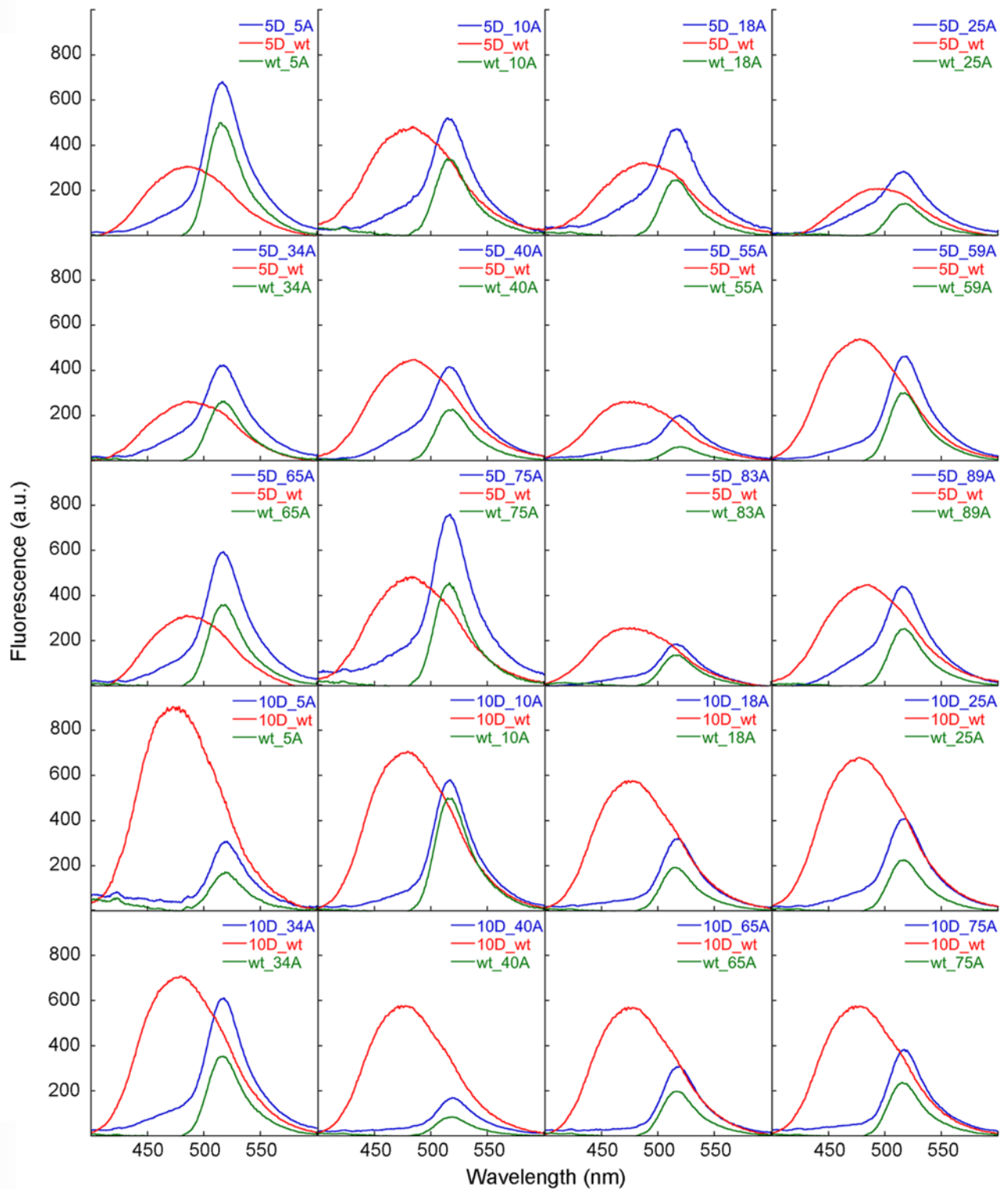


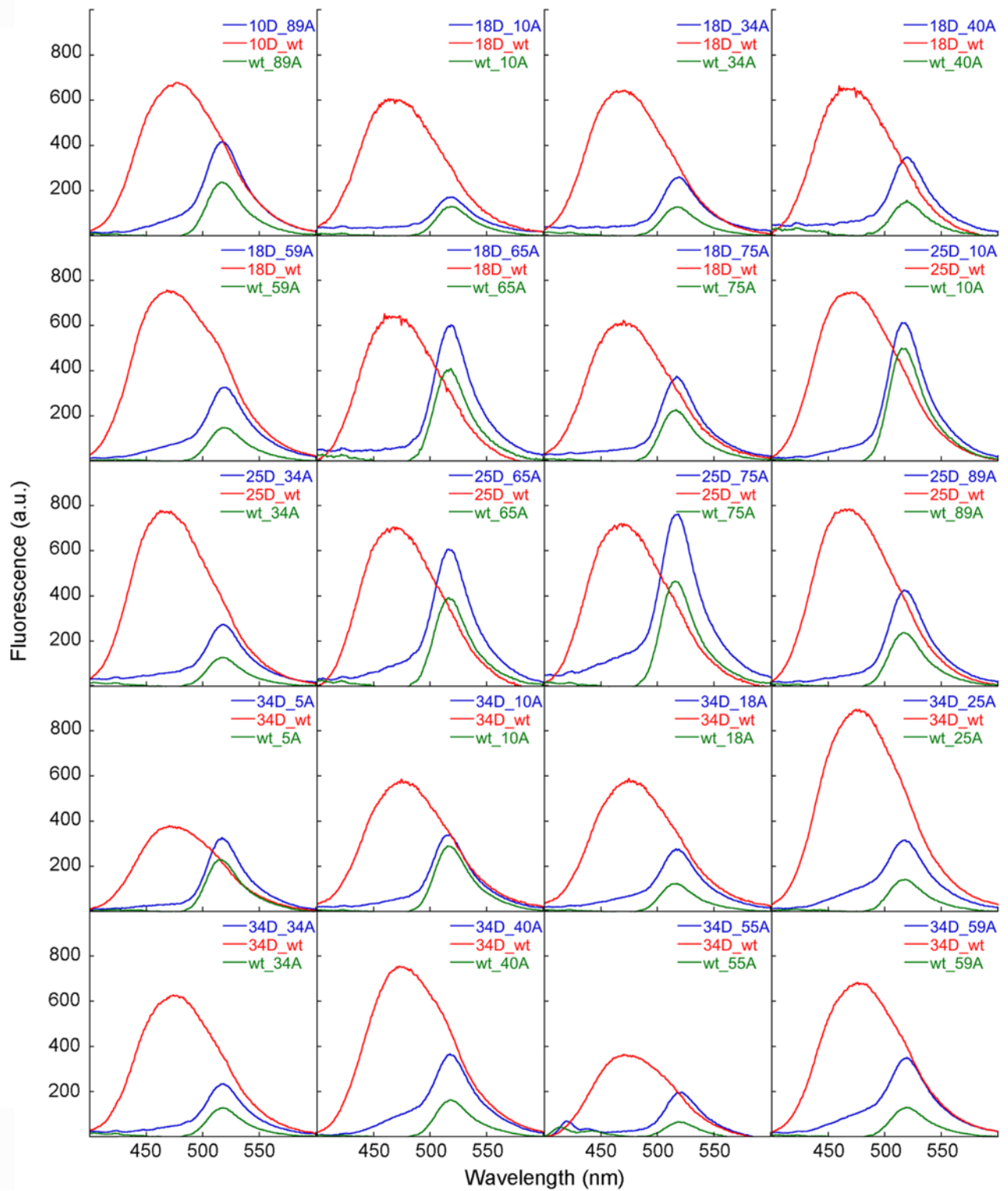
Supplementary Figure 4. (A-C) Evaluation of the effects of labelling with 1,5-IAEDANS on the oligomer structure, and (D-G) investigation of the solvent-exposure of the hydrophobic regions of type A and type B HypF-N oligomers. ThT fluorescence emission spectra (excitation 440 nm) in the presence of type A (A) and type B (B) HypF-N oligomers formed entirely by the wild-type protein (wt_wt), and by the protein labelled with 1,5-IAEDANS at position x and the wt protein in a 1:1 molar ratio (xD_wt). ThT fluorescence emission spectra of soluble GSH labelled with 1,5-IAEDANS are also

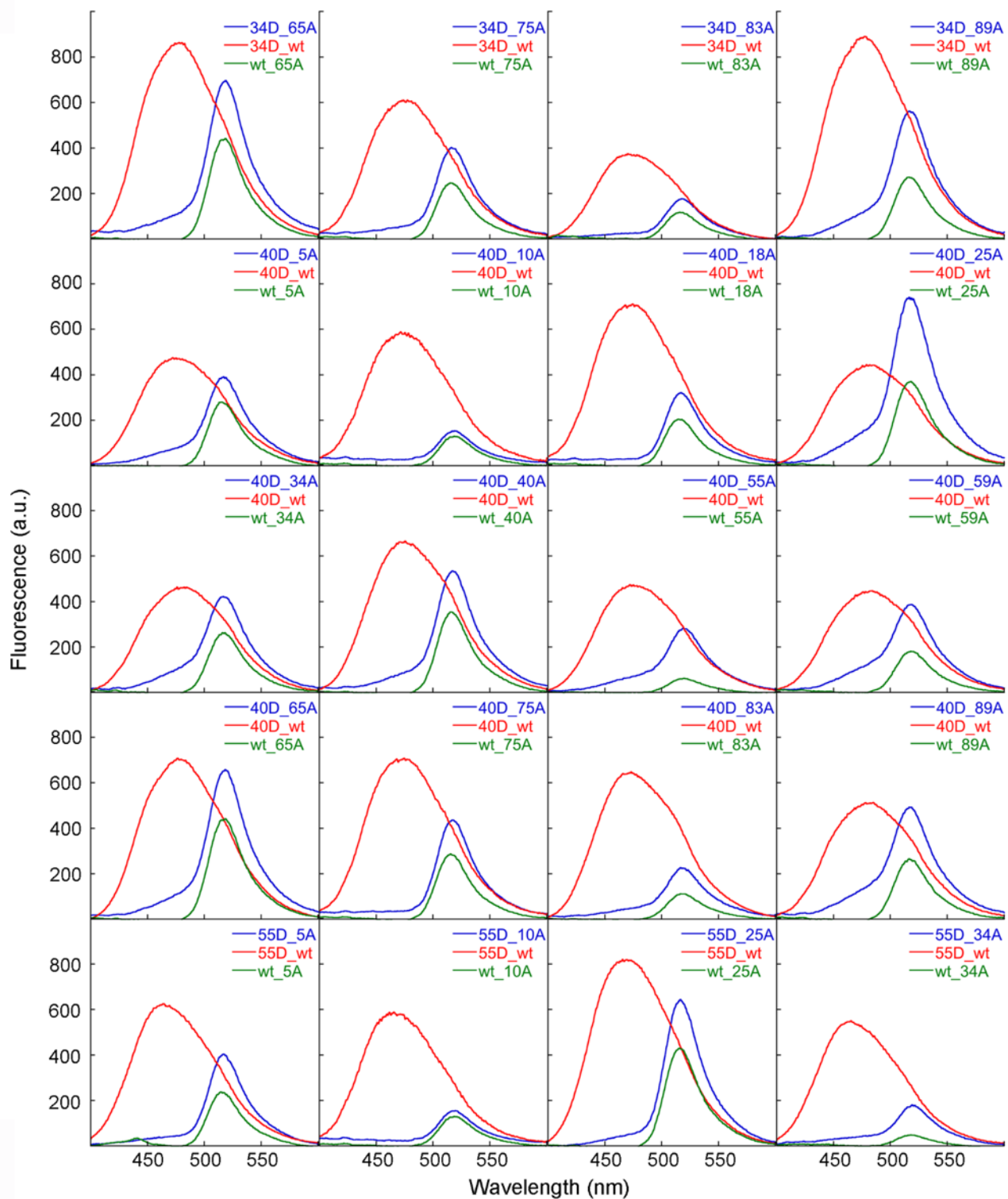
reported as a negative control (GSH-D). The fluorescence spectrum of ThT without protein was subtracted from all spectra shown in the figure. **(C)** The ThT fluorescence emission values at 485 nm for type A and type B oligomers are reported as the ratio between the ThT fluorescence in the presence (F) and absence (F_0) of samples. The data are the means \pm SD of three independent experiments. **(D)** Influence of the dielectric constant of the medium (ϵ_r) on the wavelength of the λ_{\max} of mercaptoethanol labelled with 1,5-IAEDANS.¹⁷ The analysis was carried out by dissolving 1,5-IAEDANS-mercaptoethanol in water and in several primary alcohols, and determining the λ_{\max} value for each solvent. The numbers in the figure correspond to the solvents as follows: 0 = water; 1 = methanol; 2 = ethanol; 3 = 1-propanol; 4 = 1-butanol; 5 = 1-pentanol; 6 = 1-hexanol; 7 = 1-heptanol; 8 = 1-octanol; 9 = 1-nonanol. The graph shows that the λ_{\max} of 1,5-IAEDANS is most blue-shifted in 1-butanol and is red-shifted when using both more hydrophobic (1-pentanol, 1-hexanol, 1-heptanol, 1-octanol, 1-nonanol) and more hydrophilic (water, methanol, ethanol, 1-propanol) solvents¹. The green and red linear functions describe the λ_{\max} trend when 1,5-IAEDANS is dissolved in hydrophobic (green points) and hydrophilic (red points) solvents, respectively. Panel **D** was modified from Hammarström et al., 2001.¹⁷ **(E)** λ_{\max} of 1,5-IAEDANS *versus* residue number obtained for the 12 type A (red) and type B (blue) HypF-N oligomers formed by the protein labelled with 1,5-IAEDANS at position x and the wt protein in a 1:1 molar ratio (xD_wt). The black line indicates the 1,5-IAEDANS λ_{\max} value of 470 nm typical of a protein hydrophobic core calculated by using the green function reported in **D** and the dielectric constant of the interior of a folded protein, that is approximately 4.¹⁸ Values of $\lambda_{\max} > 470$ nm (light grey region) obtained with the xD_wt oligomers indicate an environment around the 1,5-IAEDANS moiety that is more hydrophilic than the interior of a protein. By contrast, values of $\lambda_{\max} < 470$ nm (dark grey region) have a more hydrophobic environment around the 1,5-IAEDANS moiety. Residues with low values of λ_{\max} indicate that such residues experience the most hydrophobic environment in the oligomers, whereas residues with high values of λ_{\max} refer to those in the most hydrophilic environment. Since the former are below the threshold of 470 nm, the observation that such residues have lower λ_{\max} values in type A oligomers than type B oligomers indicates that the environment has a lower hydrophobicity for the type A oligomers (dark grey region). The data are means \pm SEM of a variable number of independent experiments. **(F)** Ratios between the fluorescence intensities measured at 440 nm (excimer peak) and 375 nm (monomer peak) for all the PM-labelled positions along the HypF-N sequence for type A (red) and type B (blue) HypF-N oligomers. The data are the means \pm SD of at least two independent experiments. **(G)** Hydropathy profile of HypF-N calculated using the Roseman hydrophobicity scale.¹⁹ The positions of α -helices (red) and β -strands (blue) in the native structure (protein data bank entry 1GXU) are also indicated as determined by MOLMOL.²⁰ The comparison between **E**, **F** and **G** shows that the 1,5-IAEDANS λ_{\max} profiles of the two oligomeric species are consistent with both the PM excimer ratio and the hydropathy profiles: the three most hydrophobic regions of the protein show a general blue-shift of 1,5-IAEDANS fluorescence emission and a high PM excimer ratio, indicating their burial from solvent, which appears to be less marked for type A oligomers than type B oligomers. Panels **F** and **G** are adapted from Campioni et al., 2010.¹

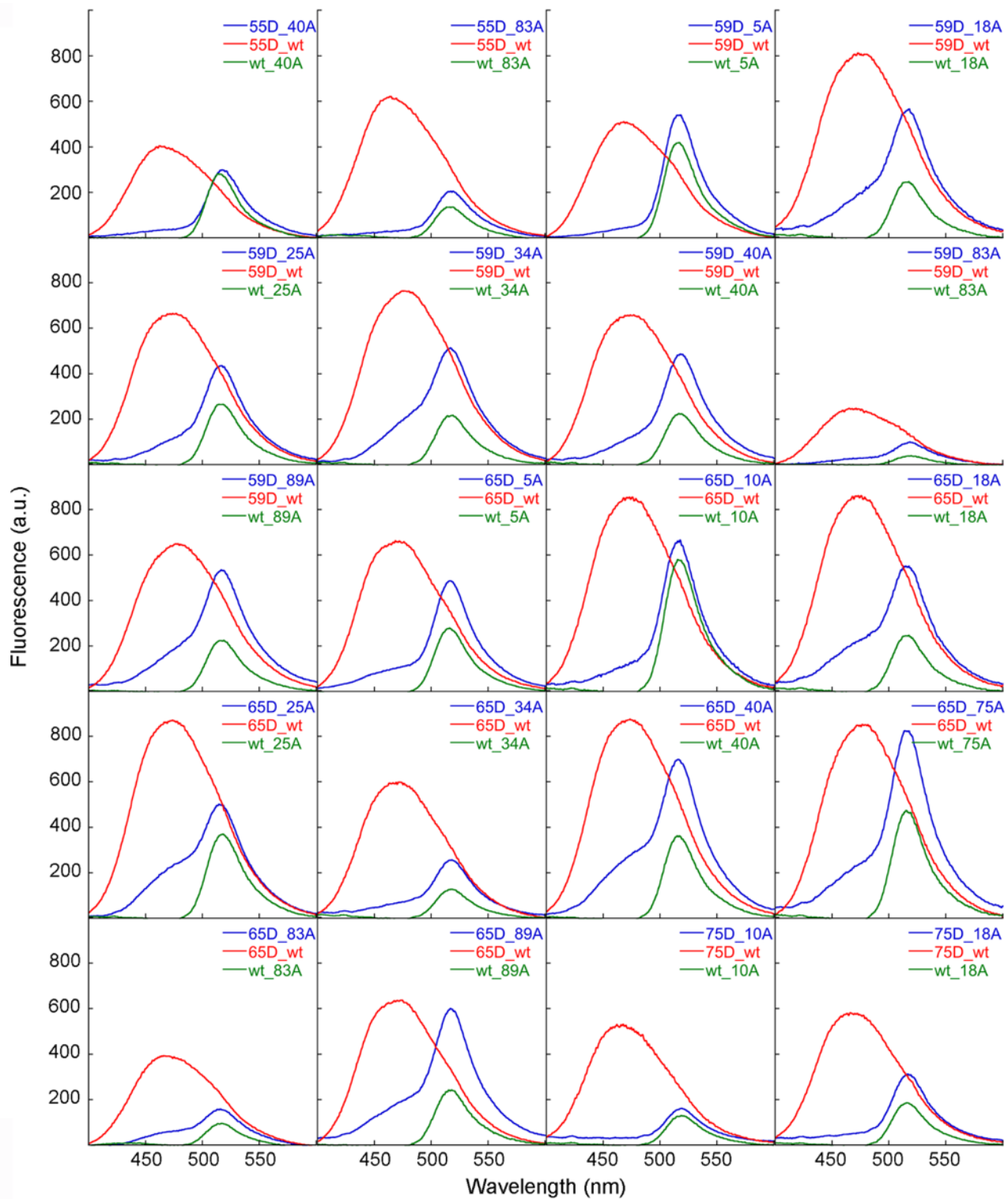


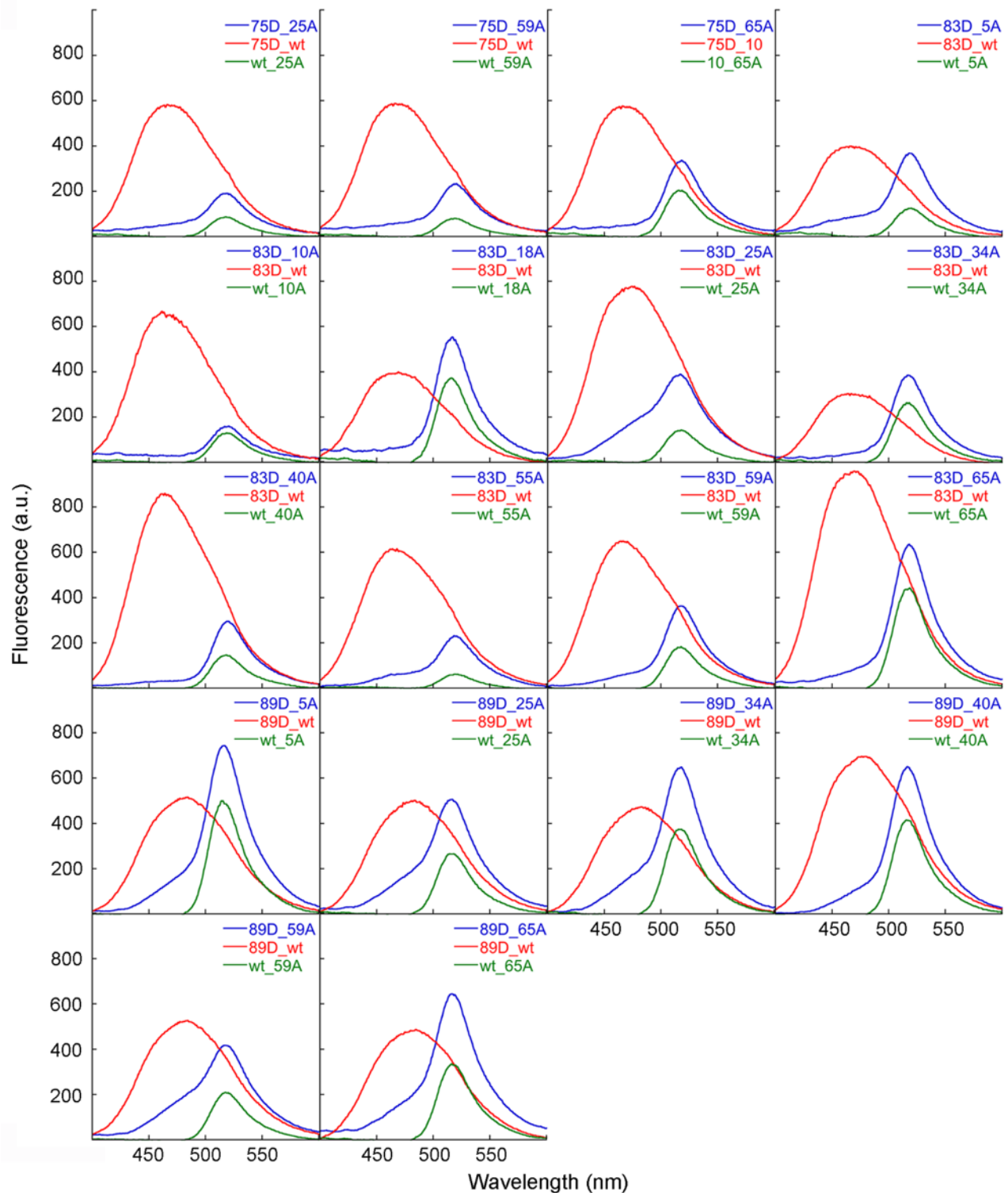
Supplementary Figure 5. Fluorescence emission spectra (excitation at 336 nm) of the native monomeric samples 65D_65A (blue spectra), 65D_65 (red spectra), and 65_65A (green spectra), where the two species are in a 1:1 molar ratio in each sample. The orange spectra represent the mathematical sum of the red and the green spectra. The samples were prepared at different protein concentrations and spectral acquisition was carried out after adequately optimising the excitation/emission (Ex/Em) slits: **(A)** 0.5:0.5 μM , Ex/Em = 2.5/4.5; **(B)** 1.0:1.0 μM , Ex/Em = 2.5/3.5; **(C)** 2.0:2.0 μM , Ex/Em = 2.5/2.5; **(D)** 4.0:4.0 μM , Ex/Em = 2.5/2.5 attenuated. In all 4 graphs, the fluorescence emission spectrum obtained in the presence of the sample 65D_65A (blue spectrum) is quite similar to the sum (orange spectrum) of the fluorescence emission spectra obtained in the presence of 65D_65 (red spectrum) and of 65_65A (green spectrum), indicating that the distance between donor and acceptor molecules in solution, when both donor- and acceptor-labelled proteins are monomeric and folded, is too high to generate any energy transfer.



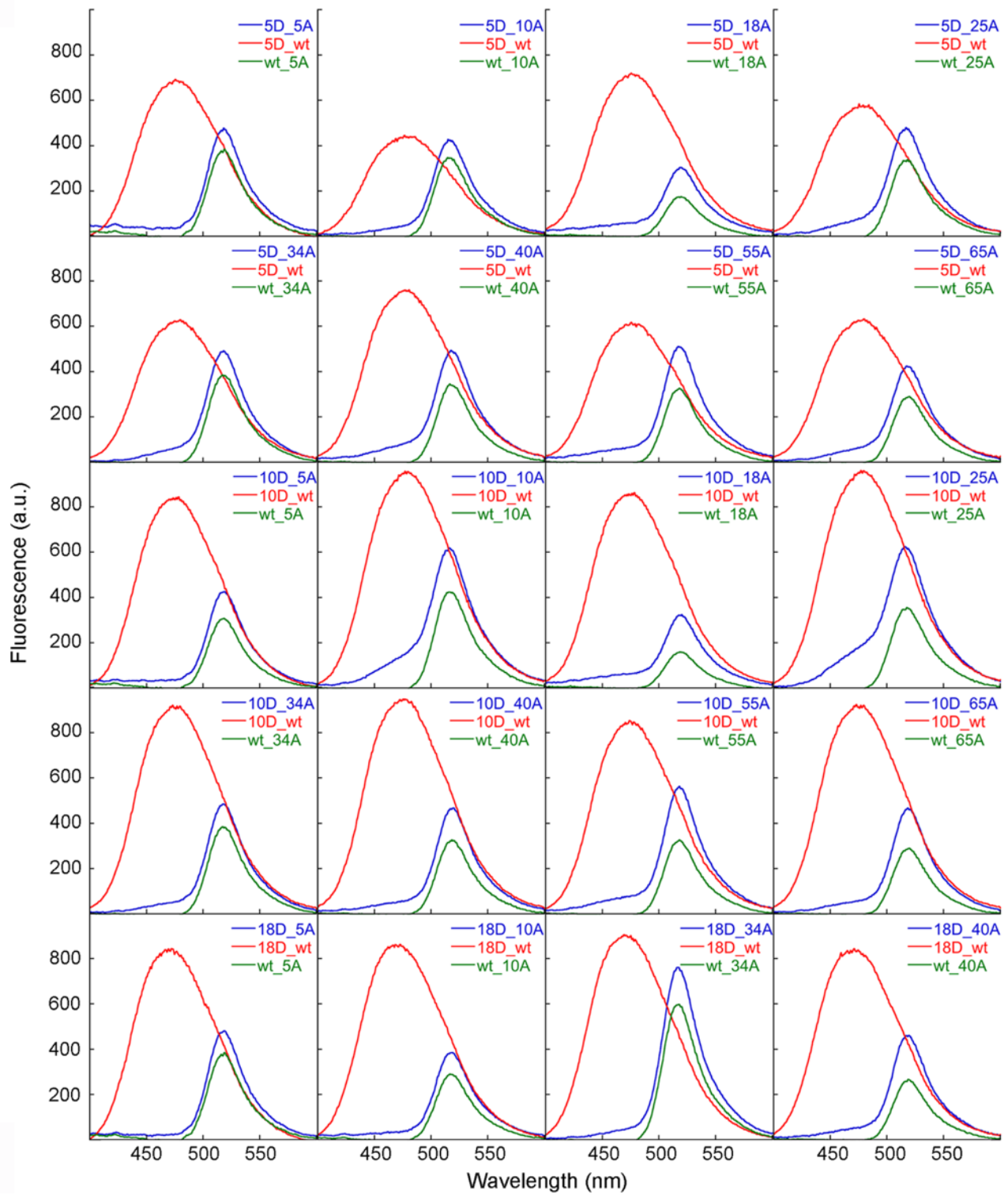


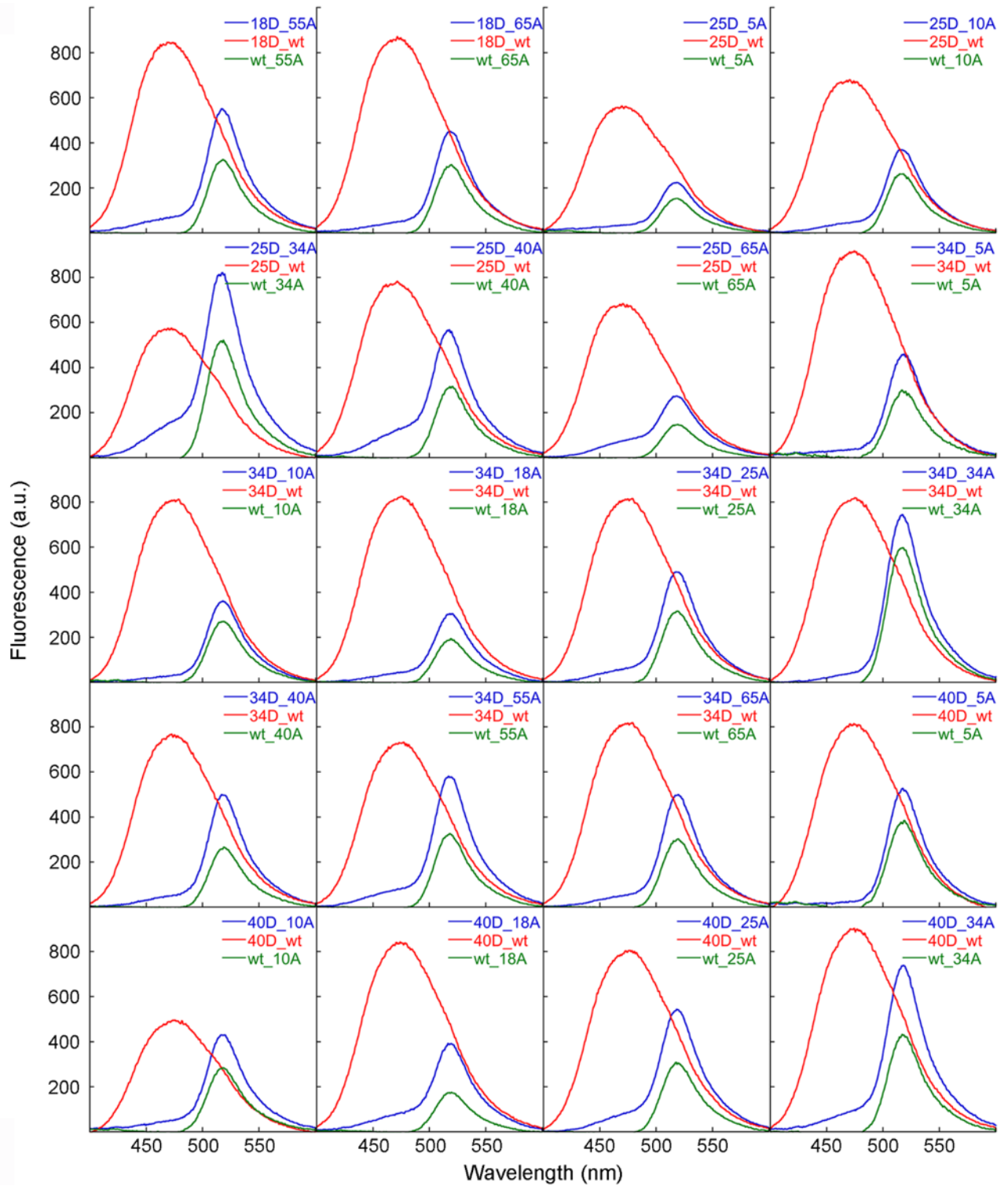


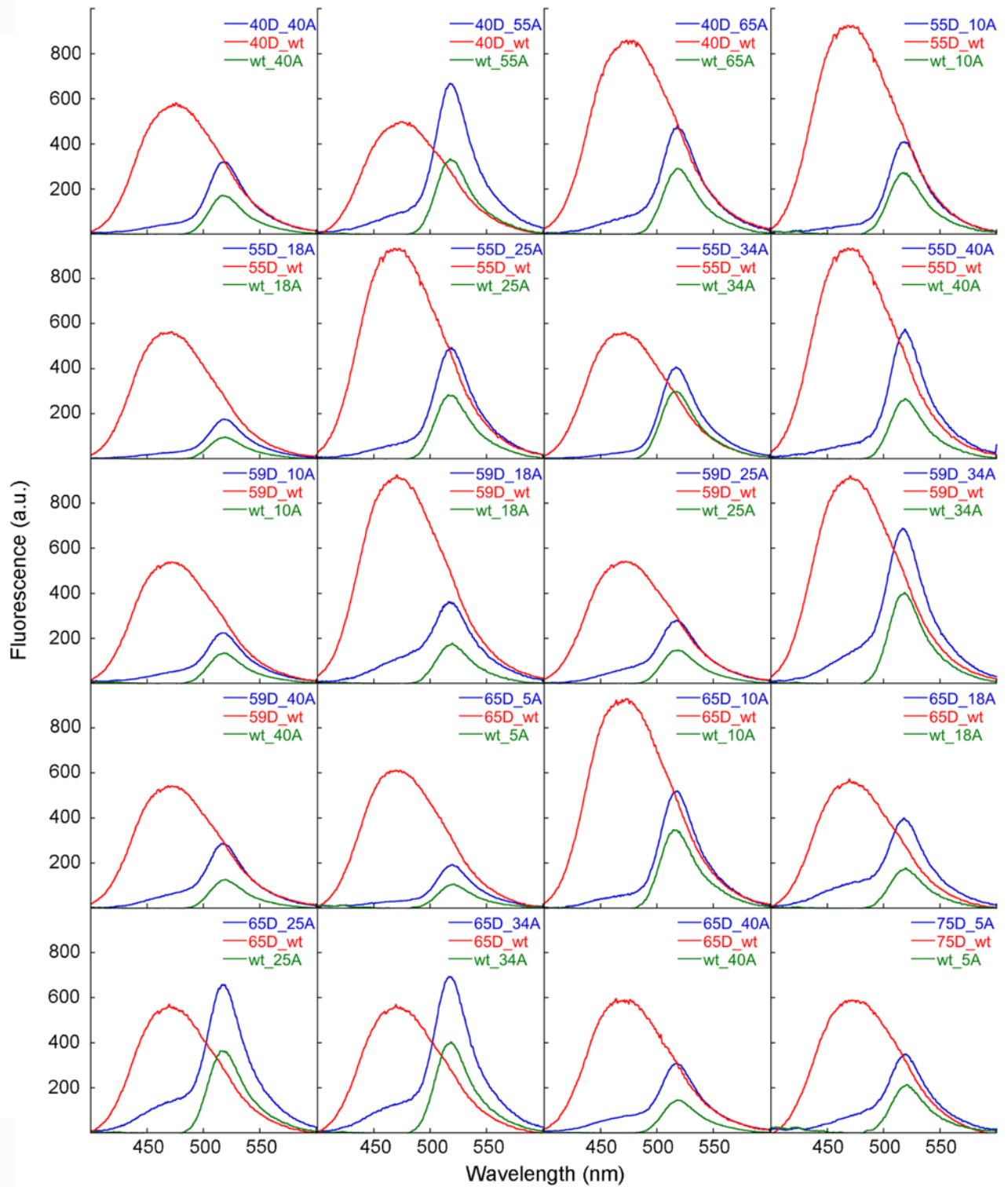


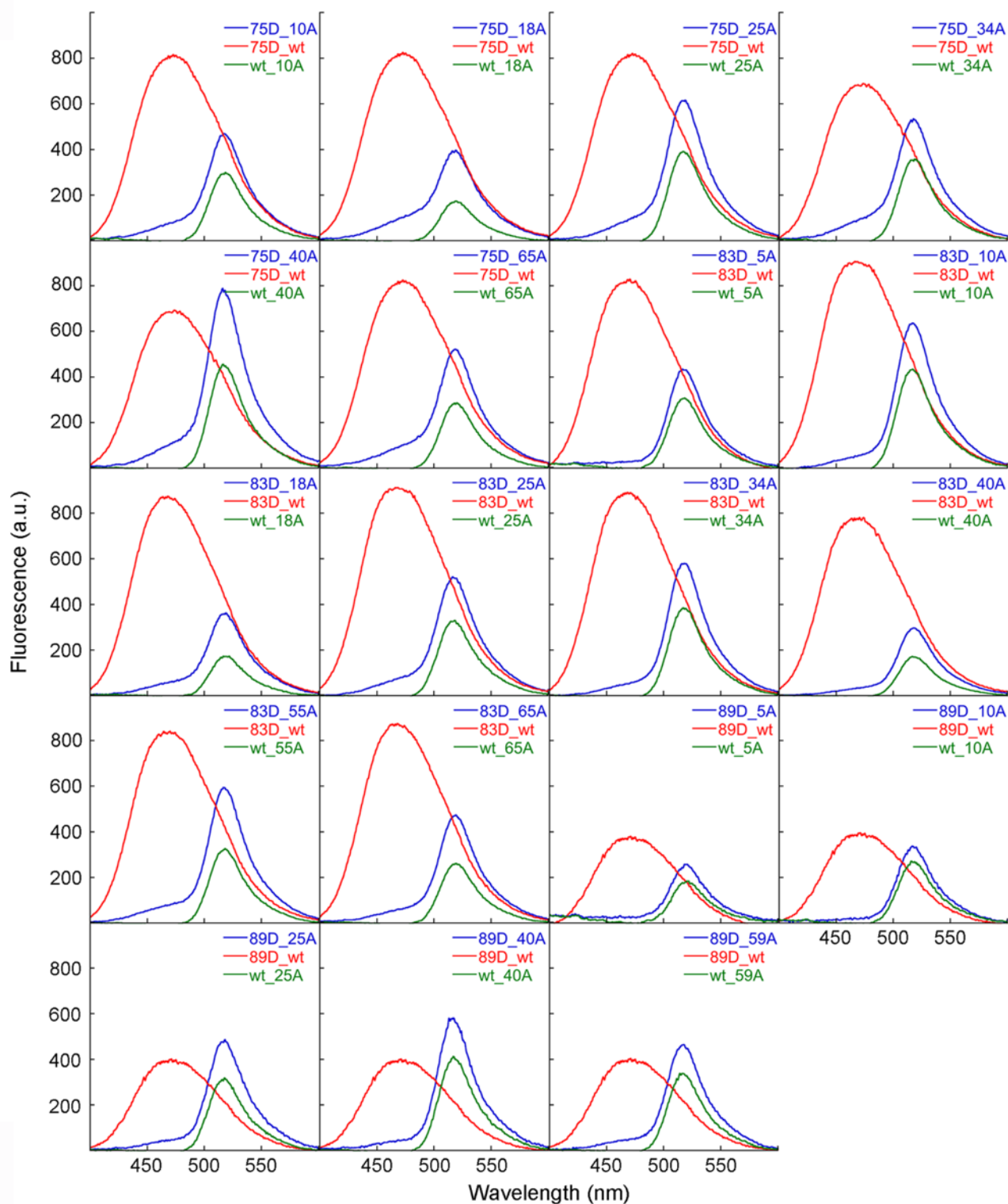


Supplementary Figure 6. Fluorescence emission spectra of the labelled HypF-N variants xD_yA (blue spectra), xD_wt (red spectra), and wt_yA (green spectra) after aggregation under condition A. The two species in each sample are in a 1:1 molar ratio. The analysis is shown for type A oligomers representing 98 pairs of donor- and acceptor-labelled variants.

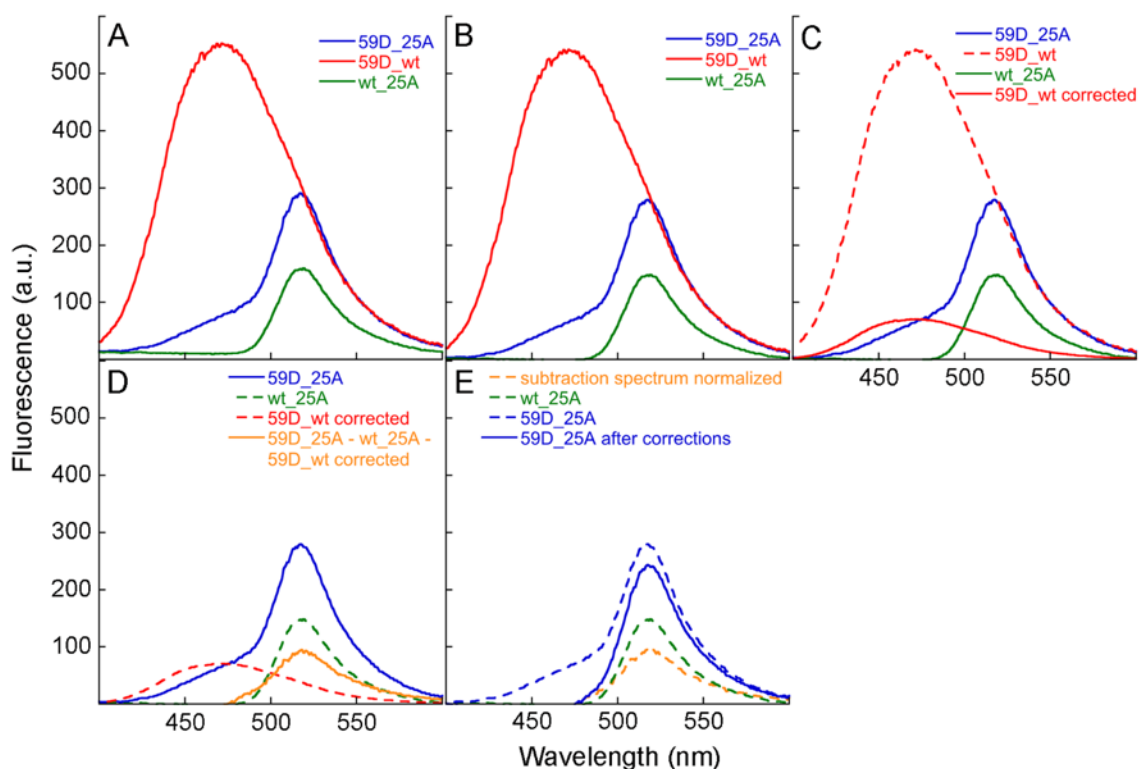








Supplementary Figure 7. Fluorescence emission spectra of the labelled HypF-N variants xD_yA (blue spectra), xD_wt (red spectra), and wt_yA (green spectra) after aggregation under condition B. The two species in each sample are in a 1:1 molar ratio. The analysis is shown for type B oligomers representing 79 pairs of donor- and acceptor-labelled variants.



Supplementary Figure 8. In order to determine the FRET efficiency between a donor-labelled residue (1,5-IAEDANS-labelled residue) and an acceptor-labelled residue (6-IAF-labelled residue) in type A and type B HypF-N oligomers, calculations were carried out for the three fluorescence emission spectra obtained in the presence of the oligomers xD_yA, xD_wt and wt_yA. As an example, the figure reports the case of the pair of mutants with the cysteine residue at positions 59 and 25 used to form nontoxic type B oligomers in a 1:1 molar ratio and labelled with donor and acceptor, respectively. **(A)** Spectra acquired using a 2 μM concentration of oligomers (59D_25A = blue line; 59D_wt = red line; wt_25A = green line). **(B)** Spectra after the subtraction of the background, determined as the fluorescence emission value at 480 nm of the spectrum obtained in the presence of the sample wt_25A. **(C)** The ratio between 59D_25A (blue solid line) and 59D_wt (red dashed line), at 475 nm emission (a wavelength at which the acceptor is not able to emit its fluorescence), has been multiplied by the spectrum 59D_wt to determine the contribution of the donor (red solid line) to the fluorescence emission of the acceptor in the spectrum 59D_25A. **(D)** The spectra relating to the contribution of the donor (red dashed line) and the acceptor (dashed green line) were subtracted from the 59D_25A spectrum (blue solid line); the difference spectrum is represented in orange. **(E)** The difference spectrum was then normalized by taking account of the degree of donor-variant labelling, which is 98% in this case, (orange dashed line). The final correction was obtained by summing the spectrum corrected by the labelling degree (orange dashed line) and the wt_25A spectrum (green dashed line), resulting in the 59D_25A spectrum (blue solid line). We calculated the FRET efficiency as $E = (I_{AD}A_A - I_{AA})/I_{AA}A_D$, where E is the FRET efficiency, A_A and A_D represent the absorbance values at 336 nm of acceptor ($A_A = 0.05$) and donor ($A_D = 0.07$), respectively, obtained in the presence of a concentration of dye of 120 μM ; I_{AD} and I_{AA} represent the acceptor fluorescence emission at 1 mM (excitation 336 nm) obtained in the presence and in the absence of donor, respectively, determined from the area between 490 nm and 600 nm below the corresponding curves (Figure S8E, blue solid line spectrum for I_{AD} and green dashed line for I_{AA}).

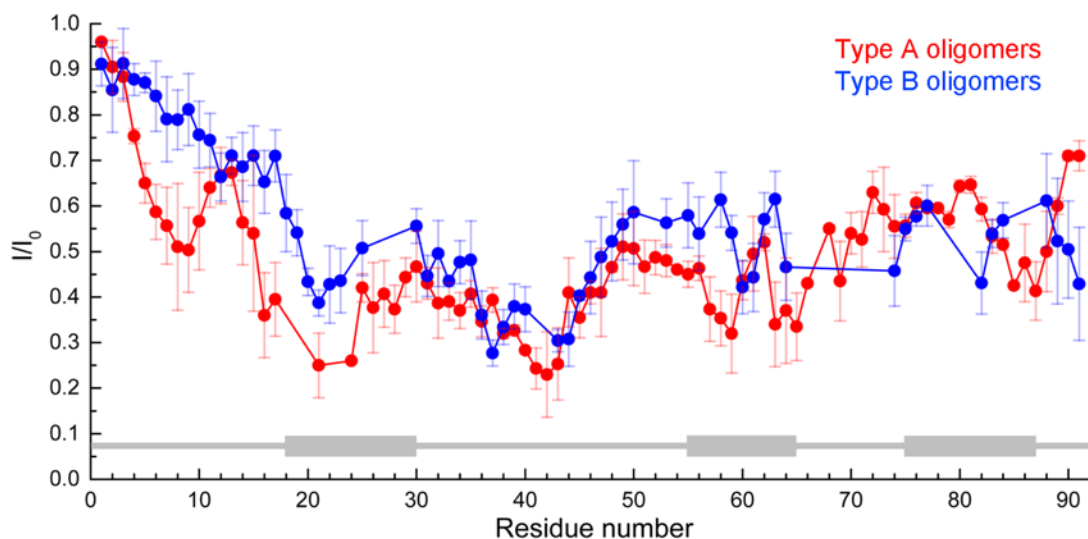
A Type A oligomers

	5A	10A	18A	25A	34A	40A	55A	59A	65A	75A	83A	89A
5D	0.39	0.52	0.89	0.49	0.53	0.38	~1	0.45	0.94	0.55	0.37	0.78
10D	0.56	0.08	0.43	0.53	0.46	0.67			0.39	0.42		0.49
18D		0.27			0.96	~1		0.90	0.45	0.47		
25D		0.18			0.76				0.35	0.40		0.72
34D	0.36	0.08	0.84	0.67	0.60	0.42	~1	0.85	0.36	0.49	0.41	0.84
40D	0.37	0.16	0.42	0.99	0.52	0.38	~1	0.86	0.35	0.40	0.81	0.97
55D	0.82	0.25		0.38	~1	0.15					0.58	
59D	0.34		0.77	0.40	0.79	0.63					~1	0.75
65D	0.52	0.06	0.72	0.05	0.70	0.54				0.42	0.42	0.91
75D		0.32	0.58	0.96				~1	0.53			
83D	~1	0.30	0.44	0.79	0.72	0.74	~1	0.79	0.36			
89D	0.42			0.60	0.36	0.41		0.62	0.80			

B Type B oligomers

	5A	10A	18A	25A	34A	40A	55A	59A	65A
5D	0.25	0.17	0.67	0.34	0.21	0.33	0.50		0.39
10D	0.30	0.19	0.71	0.32	0.18	0.32	0.50		0.46
18D	0.25	0.34			0.24	0.69	0.63		0.44
25D	0.30	0.26			0.36	0.62			0.52
34D	0.40	0.24	0.47	0.44	0.19	0.68	0.62		0.55
40D	0.28	0.35	0.84	0.53	0.44	0.59	0.72		0.38
55D		0.37	0.60	0.53	0.26	0.88			
59D		0.40	0.66	0.53	0.43	0.81			
65D	0.59	0.29	0.81	0.51	0.47	0.66			
75D	0.43	0.41	0.96	0.43	0.35	0.58			0.62
83D	0.34	0.33	0.95	0.39	0.39	0.55	0.60		0.73
89D	0.33	0.18		0.46		0.34		0.31	

Supplementary Figure 9. (A,B) FRET efficiency (E) values calculated for type A (**A**) and type B (**B**) HypF-N oligomers formed by pairs of donor- and acceptor-labelled variants. Each E value refers to the oligomer xD_yA labelled with donor and acceptor fluorophores in a 1:1 molar ratio at the positions reported on the left and above the tables, respectively (calculated as described in Figure S8).



Supplementary Figure 10. CEST profiles obtained for type A (red) and type B (blue) HypF-N oligomers. The regions of the sequence indicated by the grey bars represent the three major hydrophobic regions of the oligomers (18-30, 55-65, and 75-87). The CEST profiles obtained at ± 1.5 kHz offsets for the type A and B oligomers show a low level of saturation of the N-terminal region of the protein, particularly for nontoxic type B oligomers. In addition, the CEST profiles identify three regions (residues 15-24, 36-44, and 85-87) with high levels of saturation, indicating a similarly strong association of these regions with the slow-tumbling core of both types of oligomers. Moreover, residues 55-66 show high levels of saturation but only in the type A oligomers. The regions encompassing residues 15-24, 55-66 and 85-87 are highly hydrophobic and correspond, to a good approximation, to the regions of the sequence that represent maxima in the hydropathy profile and that are located in highly structured parts of the oligomers, as determined by the fluorescence experiments with 1,5-IAEDANS and PM (18-30, 55-65 and 75-87, Figure S4E-G). By contrast, the region comprising residues 36-44 is not hydrophobic, but may be involved in additional interactions that are not detected by the other experimental techniques. This analysis shows that the various hydrophobic regions, with the contribution of the region of residues 36-44, participate in a similar manner to the formation of the rigid regions of the two types of oligomers and are therefore likely to be directly involved in the core regions in both cases.

Acknowledgments

This work was supported by the Regione Toscana (project FAS-Salute - Supremal, FC, CDA, PM), Leverhulme Trust (RPG-2015-350, AD), the UK Biotechnology and Biological Sciences Research Council (BB/M023923/1, AD), the University of Milano-Bicocca (2015-ATE-0119, AN), the University of Genoa (FRA 2016, AR), the Cambridge Centre for Misfolding Diseases (CMD, MV), and the Department of Chemistry of the University of Cambridge (MA18512, CC). We thank Filippo Tramontana for the assistance with the table of contents graphic.

References

- (1) S. Campioni, B. Mannini, M. Zampagni, A. Pensalfini, C. Parrini, E. Evangelisti, A. Relini, M. Stefani, C. M. Dobson, C. Cecchi and F. Chiti, *Nat. Chem. Biol.*, 2010, **6**, 140.
- (2) G. Calloni, C. Lendel, S. Campioni, S. Giannini, A. Gliozzi, A. Relini, M. Vendruscolo, C. M. Dobson, X. Salvatella and F. Chiti, *J. Am. Chem. Soc.*, 2008, **130**, 13040.
- (3) A. Natalello, A. Relini, A. Penco, L. Halabelian, M. Bolognesi, S. M. Doglia and S. Ricagno, *PLoS One*, 2015, **10**, e0122449.
- (4) E. Goormaghtigh, V. Raussens and J. M. Ruyschaert, *Biochim. Biophys. Acta.*, 1999, **1422**, 105.
- (5) H. Susi and D. M. Byler, *Methods Enzymol.*, 1986, **130**, 290.
- (6) A. Natalello, D. Ami, S. Brocca, M. Lotti and S. M. Doglia, *Biochem. J.*, 2005, **385**, 511.
- (7) K. Takegoshi, S. Nakamura and T. Terao, *Chem. Phys. Lett.*, 2001, **344**, 631.
- (8) M. Baldus, A. T. Petkova, J. Herzfeld and R. G. Griffin, *Mol. Phys.*, 1998, **95**, 1197.
- (9) G. Comellas, J. J. Lopez, A. J. Nieuwkoop, L. R. Lemkau and C. M. Rienstra, *J. Magn. Reson.*, 2011, **209**, 131.
- (10) G. Bodenhausen and D. J. Ruben, *Chem. Phys. Lett.*, 1980, **69**, 185.
- (11) S. P. Skinner, R. H. Fogh, W. Boucher, T. J. Ragan, L. G. Mureddu and G. W. Vuister, *J. Biomol. NMR*, 2016, **66**, 111.
- (12) G. Morris, *Encyclopedia of Magnetic Resonance*, ed. D. M. Grant and R. K. Harris, J. Wiley and Sons, 1996, Vol. 4.
- (13) F. Delaglio, S. Grzesiek, G. W. Vuister, G. Zhu, J. Pfeifer and A. Bax, *J. Biomol. NMR*, 1995, **6**, 277.
- (14) W. F. Vranken, W. Boucher, T. J. Stevens, R. H. Fogh, A. Pajon, M. Llinas, E. L. Ulrich, J. L. Markley, J. Ionides and E. D. Laue, *Proteins*, 2005, **59**, 687.
- (15) R. Sarroukh, E. Goormaghtigh, J. M. Ruyschaert and V. Raussens, *Biochim. Biophys. Acta.*, 2013, **1828**, 2328.
- (16) J. T. Pelton and L. R. McLean, *Anal. Biochem.*, 2000, **277**, 167.
- (17) P. Hammarström, R. Owenius, L. G. Måsténsson, U. Carlsson and M. Lindgren, *Biophys. J.*, 2001, **80**, 2867–2885.
- (18) J. J. Dwyer, A. G. Gittis, D. A. Karp, E. E. Lattman, D. S. Spencer and W. E. Stites, *Biophys. J.*, 2000, **79**, 1610–1620.
- (19) M. A. Roseman, *J. Mol. Biol.*, 1988, **200**, 513–522.
- (20) R. Koradi, M. Billeter and K. Wüthrich, *J. Mol. Graph.*, 1996, **14**, 51–55.